1990 SCA CONFERENCE PAPER NUMBER 90002

Pore Image Characterization and Its Relationship to Permeability

by

Li-Ping Yuan
Alberta Research Council, P.O. Box 8330, Station F,
Edmonton, Alberta T6H 5X2

Petrographic image analysis has the potential to estimate flow properties of a reservoir rock by analyzing its pore geometry and pore structure. This analysis can be performed on samples which are too small for conventional flow experiments. Special image analysis algorithms have been used to measure pore size distributions and pore connectivities from two-dimensional pore images and the results have been related to measured permeability data.

The pore size distribution in a plane section is derived from an erosion-dilation algorithm which eliminates the identification of individual pore bodies. Such identification can be very subjective and difficult for highly irregular and interconnected pore images. The concept of pore sizes measured by the erosion-dilation algorithm is similar to the concept of throat sizes measured by the mercury injection method.

In order to evaluate the pore connectivity, which is important to many petrophysical properties, the pore area is divided into smooth and rough components. For each two-dimensionally isolated pore area, the smooth component is approximately the area of the largest inscribed circle and the rough component is the remaining pore area. An indicator is then defined as the ratio of the total rough components to the total pore area. A value of zero corresponds to isolated circular pores and as the indicator approaches one, the pore image typically consists of highly interconnected pores. Therefore, this indicator is used as a measure of pore connectivity in this study.

Petrographic image analysis has been used to analyze the pore images of unconsolidated sands from a heavy oil reservoir in east central Alberta, Canada. The mean pore size and the connectivity indicator were found to be strongly correlated with measured permeability. This correlation suggests a new method of predicting permeability from small samples and confirms that important aspects of the three-dimensional pore geometry information can be effectively measured from two-dimensional images. The effects of small scale heterogeneities, such as horizontal laminae, were also observed while relating pore data to permeabilities. In addition, pore size and connectivity are closely associated to the depositional environment and later diagenesis; as a result, the geological information can be more effectively used for reservoir characterization.

Introduction

Petrographic image analysis has been used in the study of two-dimensional (2-D) pore geometry in order to understand and to predict the fluid flow properties, such as permeability, of porous media (Matheron, 1967; Rink and Schopper, 1978; Ehrlich et al, 1984; Ruzyla, 1986; Berryman and Blair, 1986; Doyen, 1988; and Ehrlich and Davies, 1989). This analysis has the potential to estimate flow properties from small samples such as drilling cuttings, and to obtain flow information as a less expensive and/or a faster method than certain special core analyses.

Many different approaches can be used to analyze a binary image which is composed of either pore or non-pore pixels (picture elements). The porosity and surface area can be obtained by directly measuring pore area and perimeter or by indirectly measuring a two-point correlation function on an image (Berryman and Blair, 1986). These two parameters can, theoretically, be used to predict permeability by using a Kozeny-Carman type of equation (see Walsh and Brace, 1984, for a review). However, the surface area measured from pore images is usually a function of resolution (i.e. magnification) and therefore choosing an adequate magnification becomes crucial to the permeability prediction.

Other measurements such as size, shape, and connectivity are more difficult to obtain and even to define because of the interconnectedness of the pore network. In three dimensional (3-D) space, all effective porosity is interconnected. Three-dimensional isolated pores are less interesting due to their irrelevance to fluid flow. However, the three-dimensionally connected effective porosity is not necessarily interconnected on a 2-D image. The 2-D connectivity varies from highly connected pore images of unconsolidated materials to the highly disconnected 2-D porosity of certain consolidated materials. Because of the difficulty in defining a single pore object, some conventional size measurements such as Feret's diameter (Feret, 1931), and Wadell's diameter (Wadell, 1932) become questionable. A 'cutting' algorithm (Rink, 1976) has been used to disconnect the pore network and analyze the isolated pieces of porosity. However, it is felt that much of the information is probably altered or lost during the 'cutting' process.

In this paper, a generalized size analysis is used to measure the pore size distribution and the fraction of rough pore areas (Ehrlich et al., 1984) is used as a connectivity indicator. These size and connectivity measurements are then applied to a pore system study of a heavy oil reservoir.

Generalized size analysis

Delfiner (1972) defined a generalized concept of size which does not require a predefined single object and is especially suitable for irregularly shaped and/or interconnected objects such as pore images. He

used a series of "opening" image processing operations to perform the analysis. An opening with a circular structuring element of radius r is to remove a strip of porosity with the width r along the pore boundary (erosion) and then to add a strip of porosity with the same width back on the pore (dilation), if the pore remains (Figure 1). Small features are removed and can not be recovered, whereas large features shrink and then expand to their original size. With different sizes of structuring elements, features with various sizes can then be identified by performing a series of opening operations.

Mathematically speaking, the size measurement of each point of pore area is equal to the radius of the largest inscribed circle which contains the point and lies entirely within the pore area. This size definition was suggested by Scheidegger (1960) to characterize pore size; however, a practical measuring technique was not available until the recent development of computerized image analysis. This generalized size analysis is closely related to the mercury porosimetry analysis which measures the saturation versus the radius of the interface curvature at a given pressure. This is similar to measuring the remaining porosity versus the radius of the structuring element for a given opening operation in the generalized size analysis.

Size analysis based on performing conventional opening processes on a digital computer is very slow, especially for large objects which require many opening operations and large structuring elements for the later operations. A significant improvement to the algorithm can be made by replacing a conventional opening operation by a series of one unit erosions followed by the same number of one unit dilations. One unit erosion (or dilation) is to remove (or add) a single pixel layer. A series of unit erosions or dilations with a small structuring element is much more efficient than an equivalent erosion or dilation of a thick layer with a large structuring element. Furthermore, it is not necessary to start eroding from the original image in each opening step. Each eroded image can be saved in the computer memory. At the beginning of the next opening, the previously eroded image can be retrieved and applied with a unit erosion to complete the erosion half of the opening process. A detailed discussion on this subject has been presented by Yuan (in press) and a simplified flow chart with example images is shown in Figure 2. Several "erosion-dilation" based algorithms have been developed to perform the generalized size analysis (Rink, 1976; Parker, 1988; Crabtree et al., 1990).

Connectivity indicator

A two-dimensionally connected area of porosity can be defined as a 'porel' (pore element). Thus, for a completely connected 2-D pore image, only one porel is observed. Many porels on an image means that the 2-D porosity is distributed into many disconnected areas. Therefore, the number of porels in an image could be used as a measure of pore connectivity ('connectivity number', Serra, 1982). However, this number does not consider the weight

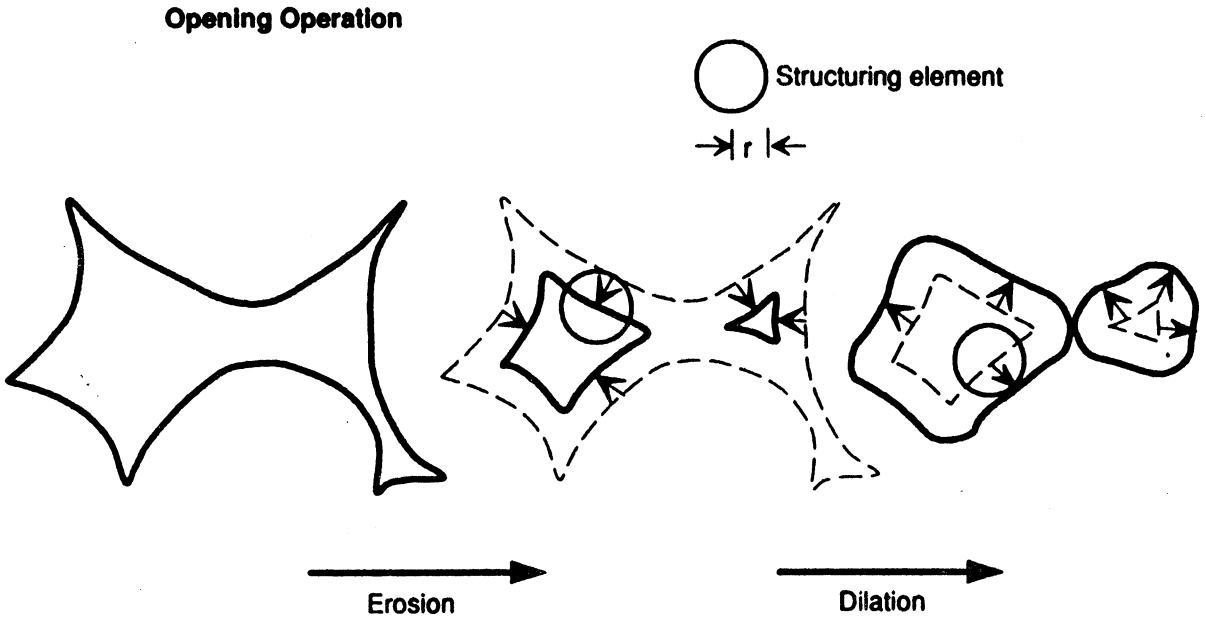

Figure 1.- Opening with a disk of radius r.

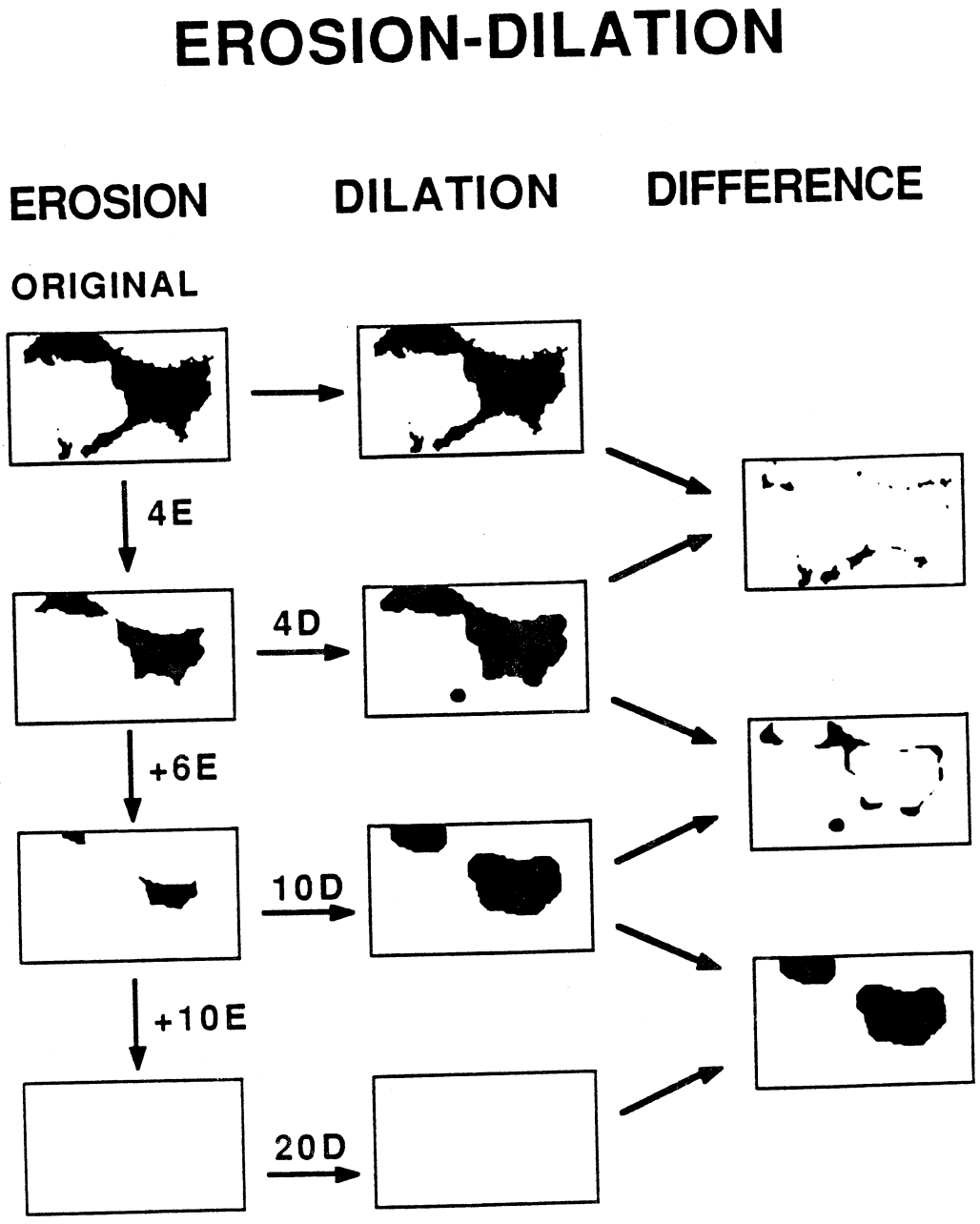

Figure 2.- Erosion-dilation image processing algorithm. Dilated images represent a sequential loss of porosity from small features to large features. This is used as a size distribution by measuring the differences between subsequent dilated images.

of porosity. A highly connected 2-D pore image may have many small (e.g. one pixel) porels associated with it. These small porels are not very important in terms of flow due to the small amount of porosity, but they result in a large porel count which indicates a disconnected pore image.

Ehrlich et al (1984) have classified porosity into smooth and rough components. The original attempt was to separate the major portion of the pore (pore body) from the pore wall roughness (Figure 3). The smooth component is the portion remaining until the last opening process which totally removes (erodes) the porel. In other words, the smooth component is all the pixels which have the largest pore size measurement (as described in the previous section) of a porel. The smooth porosity is usually, but not always, the area of the largest inscribed circle of a porel. The other portion of the porosity of a porel is then classified as the rough component.

This concept of smooth and rough porosity works well for a porel with only one significant major pore body such as the one shown in Figure 3. However, it loses its original meaning of distinguishing pore body and pore wall roughness when several pore bodies are interconnected. For a porel with several significant pore bodies, only the largest one can be the smooth component. Thus, as a result of smaller number of porels, the smooth component of a highly connected pore image is much smaller than the smooth component of a disconnected pore image. In this study, instead of using smooth porosity which increases as connectivity decreases, the ratio of rough porosity to total porosity is chosen as a connectivity indicator (Figure 4). This ratio is based on porosity measurements which are less sensitive to certain noises such as one pixel porels.

The Provost Upper Mannville B Pool

Detailed reservoir characterization is an essential part of a successful enhanced oil recovery project. An integrated reservoir analysis study (Kramers et al., 1989) is in progress for the Provost Upper Mannville B Pool of east central Alberta. One aspect of this study is to characterize the pore systems in sandy portions of this heavy oil reservoir in order to investigate the relationships between geological facies, pore systems and petrophysical properties.

The Provost Upper Mannville B Pool is contained in McLaren Formation channel sands of Lower Cretaceous age and can be subdivided into blocky channel, shale clasts and channel margin facies (Figure 5). The sands are relatively clean, quartzose, medium to fine-to-medium grained sands. Towards the top of the reservoir they become finer grained and show a slight increase in the amount of silt and clay. Net pay averages 10-12 m with a maximum of 26.5 m and parts of the reservoir have an underlying water leg up to 8 m thick. A detailed discussion of the facies and regional geology is presented by Kramers et al.(1989). The influence of the highly heterogeneous shale clast zones on fluid flow is discussed in detail by Cuthiell et al. (in press).

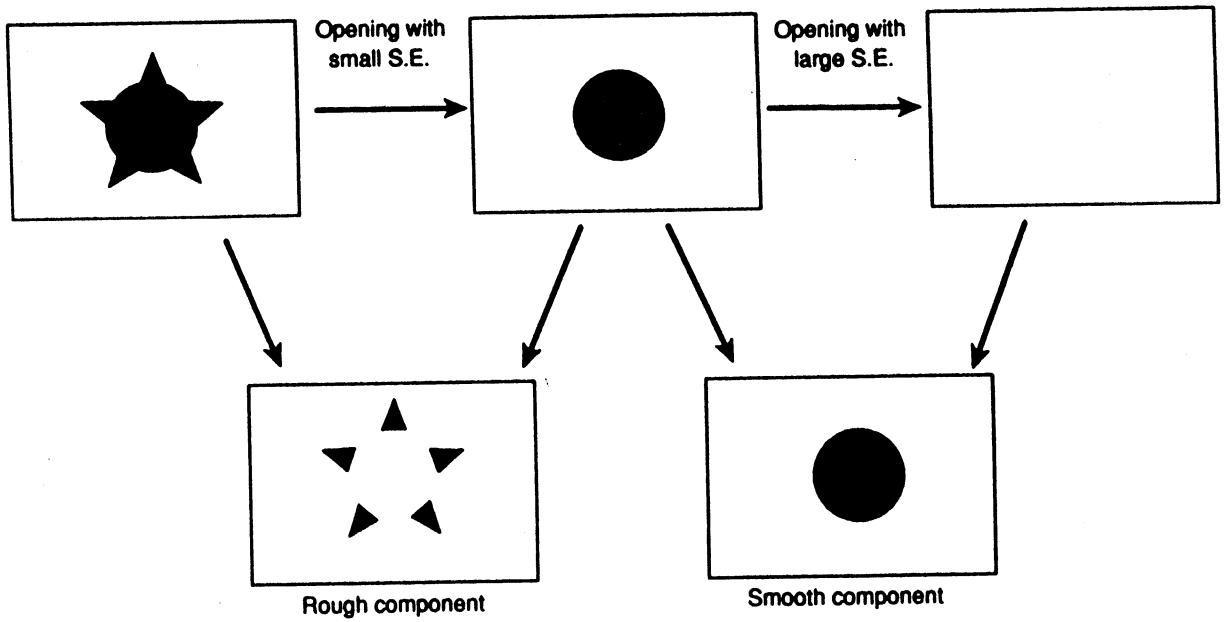

Figure 3.- Opening processes remove the rough component (pore wall roughness) first, the last opening process for a porel removes the smooth component of the porel (modified from Ehrlich et al., 1984).

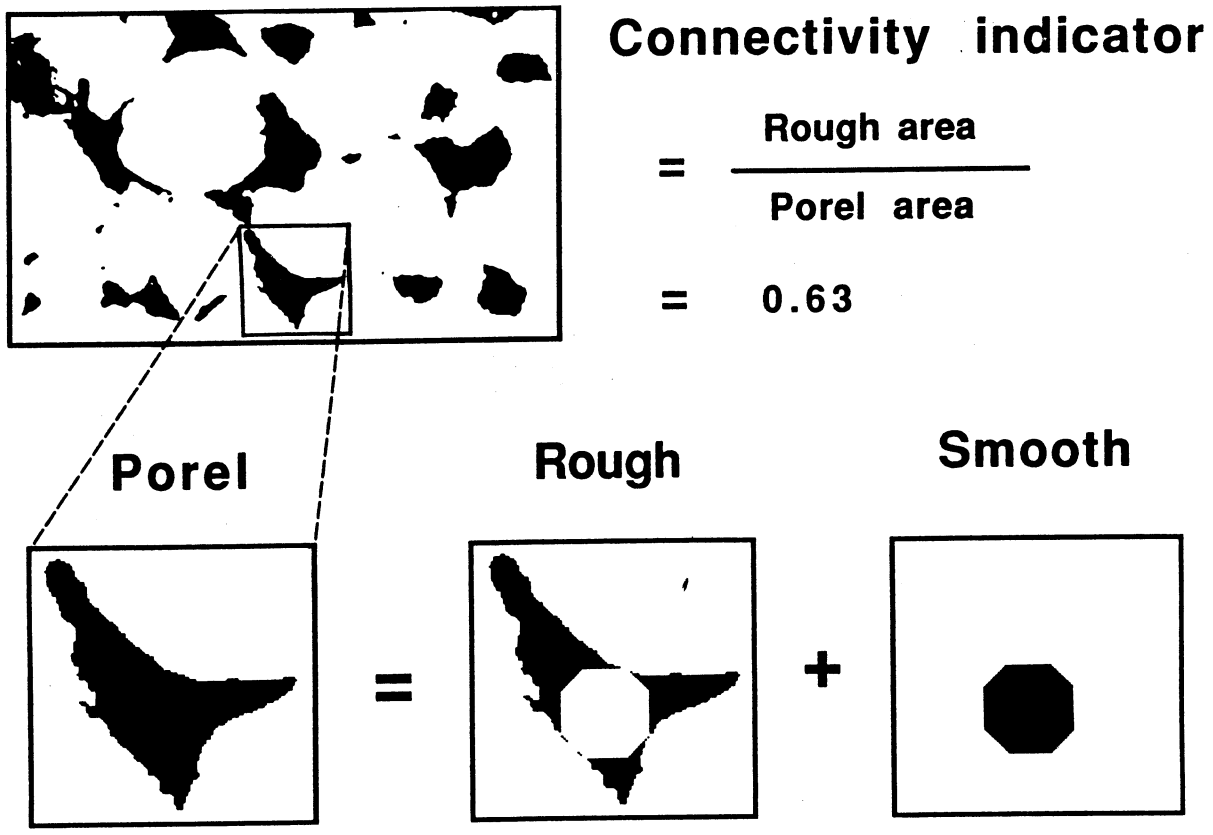

Figure 4.- A porel (pore element) is a discrete unconnected patch of porosity. The smooth component is the portion with the largest size which resembles an inscribed circle of the porel. The rest of the porel is rough component. The ratio of the rough component to the porel area is defined as a connectivity indicator.

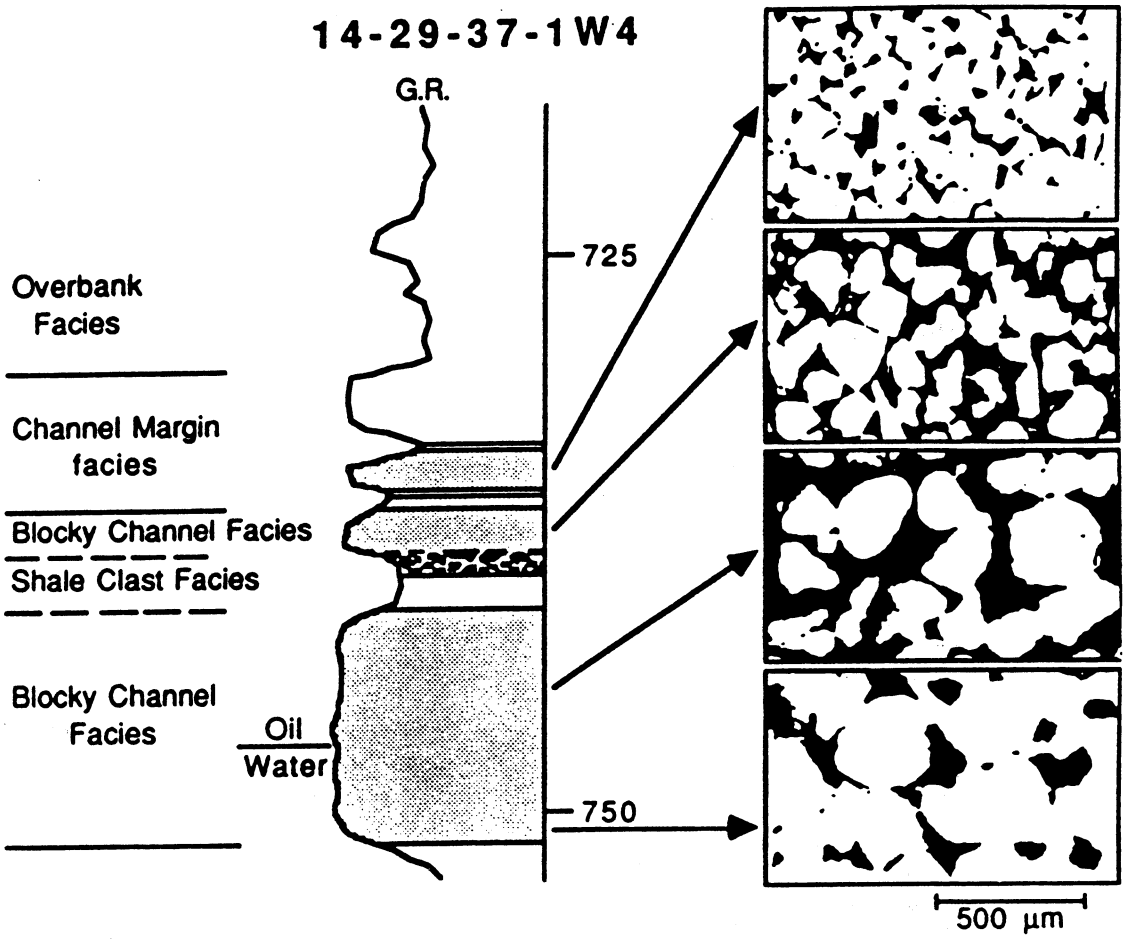

Figure 5.- Reservoir lithofacies and their characteristic pore end members.

Twenty-two horizontal plugs were taken from the blocky channel and channel margin facies from six cored wells in the reservoir. All samples were confined by either lead sleeves or teflon tubes prior to the toluene extraction of heavy oil. Horizontal permeabilities were then measured on 19 samples under overburden pressure. Samples were later impregnated with epoxy and petrographic thin sections were made. The epoxy had been mixed with a fluorescent dye to facilitate the identification of pore/grain area with a fluorescent microscope (Gies, 1987). Two thin sections, one vertical and one horizontal, were made from each plug.

A video camera mounted on top of the microscope acquires and transmits thin section images to a computer. An intensity threshold value is chosen to distinguish the bright pore areas from the dark mineral grains and binary images are produced. The erosion-dilation image processing technique is then applied to each image to produce a generalized size distribution which can be further divided into a smooth and a rough size distributions. Figure 6 shows four images and their smooth and rough size distributions. Sixteen images are digitized per thin section and the image analysis measurements are averaged for each thin section. The mean of the generalized size distribution is used as a single value for pore size and the fraction of rough pore component is used as a connectivity indicator. The smooth and rough size distributions are then analyzed by an unmixing procedure (Full et al, 1984; Full et al, 1981) to represent each sample as composed of a number of end members. The main results are listed in Table 1.

A quantitative relationship between measured permeabilities and image data can be established by regression analysis. This can then be used to predict permeability for samples where no permeability measurements are available. In this study, horizontal permeabilities are correlated to both horizontal thin section measurements and vertical thin section measurements. The results indicate that permeabilities are highly related to pore size and connectivity (Figure 7). Both regression relationships are significant at the 5% level.

The vertical thin sections provide a better pore geometry - permeability relationship than the horizontal thin sections. This is probably the result of horizontal laminae, which are better sampled by a vertical thin section. The horizontal thin section may cut through only one or possibly a few of the many laminae in an one inch diameter horizontal plug, whereas the vertical thin section cuts through all the laminae.

An unmixing procedure (Full et al., 1984; Full et al., 1981) was used to identify the pore systems of the Provost Upper Mannville B Pool reservoir. This procedure includes a Q-mode factor analysis with an iterative process to represent each sample as composed of several end members. The number of end member is chosen in a way that most of the variance of the size distributions can be explained. The results significantly simplify the large amount of image data and make it easier to interpret. Four end members were identified using this unmixing procedure, and the pore images in Figure 5 and 6 present the closest real image examples of these four hypothetical end members. In general, end member one represents large, highly connected pores; end member two represents medium size and highly connected pores; end member three is medium-large sized but isolated pores;

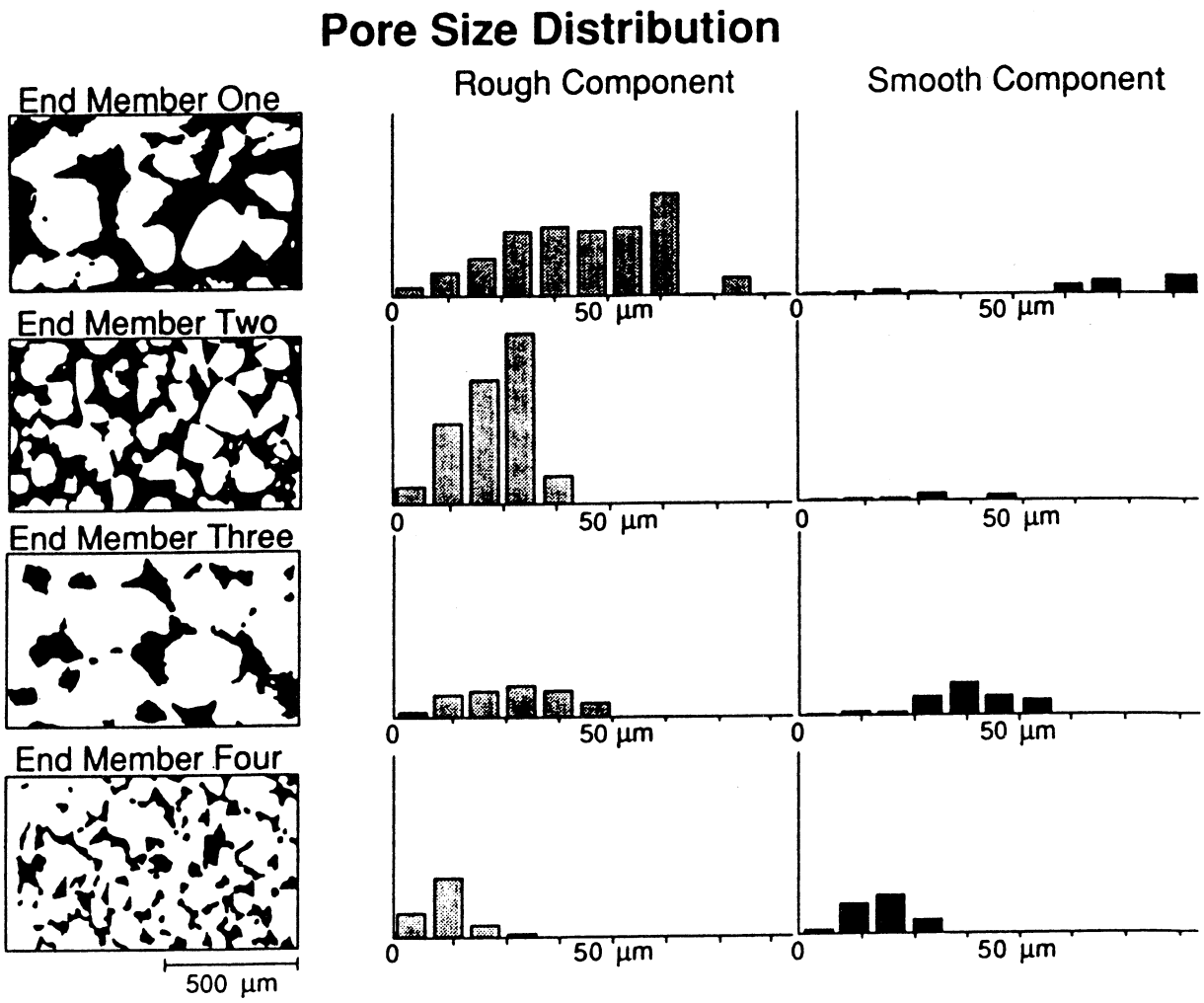

Figure 6.- Representative end member images with their rough and smooth size distributions. The mean pore sizes of the four images are 45, 22, 31, and 13.5 microns; and the connectivity indicators are 0.90, 0.96, 0.59, and 0.53 respectively.

TABLE 1- Pore system analysis data. TRANS. indicates the transition between blocky channel (BLOCKY) and channel margin (MARGIN) facies sands; (W) represents water saturated sands; and End Members 1 - 4 are the pore volume fractions of end members in each sample.

SAMPLE NO.	ORIENT.	FACIES	EM1	EM2	EM3	EM4	K_h (Darcy)	Conn. Indic.	PORE SIZE(μ)
1	H	BLOCKY	**0.19**	0.57	0.17	0.06	12.1	0.83	30.4
	V		**0.19**	0.54	0.16	0.12		0.82	29.7
2	H	TRANS.	0.06	**0.63**	0.16	0.15	3.9	0.85	24.3
	V		0.05	**0.44**	0.14	0.37		0.78	21.2
3	H	MARGIN	0.02	0.55	0.12	**0.31**	2.9	0.84	20.3
	V		0.02	0.34	0.15	**0.49**		0.72	19.2
4	H	TRANS.	0.11	**0.63**	0.19	0.07	6.5	0.83	27.2
	V		0.05	**0.54**	0.20	0.21		0.77	24.3
5	H	BLOCKY	**0.40**	0.40	0.13	0.07	11.1	0.82	38.3
	V		**0.31**	0.41	0.22	0.06		0.74	36.5
6	H	BLOCKY(W)	0.20	0.45	**0.26**	0.09	5.8	0.71	33.1
	V		0.15	0.43	**0.30**	0.12		0.65	30.9
7	H	BLOCKY(W)	0.24	0.50	**0.17**	0.08	.	0.80	32.2
	V		0.05	0.43	**0.32**	0.20		0.63	26.3
8	H	BLOCKY	**0.52**	0.39	0.02	0.07	.	0.94	41.0
	V		**0.34**	0.43	0.18	0.06		0.79	36.7
9	H	MARGIN	0.16	0.59	0.14	**0.11**	.	0.85	28.1
	V		0.05	0.09	0.18	**0.67**		0.59	18.9
11	H	BLOCKY	**0.29**	0.57	0.14	0.00	11.9	0.88	33.4
	V		**0.29**	0.56	0.13	0.02		0.87	33.3
12	H	BLOCKY	**0.18**	0.57	0.18	0.07	9.2	0.81	30.4
	V		**0.11**	0.63	0.20	0.06		0.82	27.3
13	H	TRANS.	0.07	**0.64**	0.18	0.11	7.8	0.84	25.0
	V		0.03	**0.62**	0.20	0.16		0.81	23.5
14	H	BLOCKY	**0.30**	0.54	0.14	0.02	11.6	0.86	34.1
	V		**0.27**	0.54	0.14	0.04		0.85	32.5
15	H	TRANS.	0.11	**0.51**	0.20	0.19	7.9	0.76	26.2
	V		0.06	**0.66**	0.18	0.09		0.84	25.0
16	H	MARGIN	0.04	0.16	0.09	**0.72**	2.0	0.70	15.9
	V		0.03	0.31	0.11	**0.55**		0.74	17.6
17	H	TRANS.	0.02	**0.27**	0.13	0.57	3.5	0.71	18.0
	V		0.01	**0.49**	0.13	0.37		0.80	19.6
18	H	BLOCKY	**0.08**	0.57	0.21	0.14	8.8	0.79	25.7
	V		**0.12**	0.67	0.19	0.03		0.85	28.1
19	H	BLOCKY	**0.09**	0.61	0.22	0.09	7.9	0.79	26.8
	V		**0.10**	0.62	0.18	0.11		0.83	25.9
20	H	BLOCKY	**0.14**	0.50	0.17	0.19	8.0	0.80	27.1
	V		**0.23**	0.43	0.17	0.17		0.77	31.0
21	H	BLOCKY	**0.32**	0.53	0.14	0.01	11.6	0.86	35.1
	V		**0.45**	0.40	0.10	0.05		0.84	39.2
22	H	BLOCKY(W)	0.18	0.41	**0.33**	0.08	2.1	0.62	34.0
	V		0.14	0.44	**0.37**	0.05		0.61	32.3
23	H	BLOCKY(W)	0.15	0.42	**0.34**	0.10	4.1	0.62	31.8
	V		0.14	0.47	**0.30**	0.09		0.67	31.1

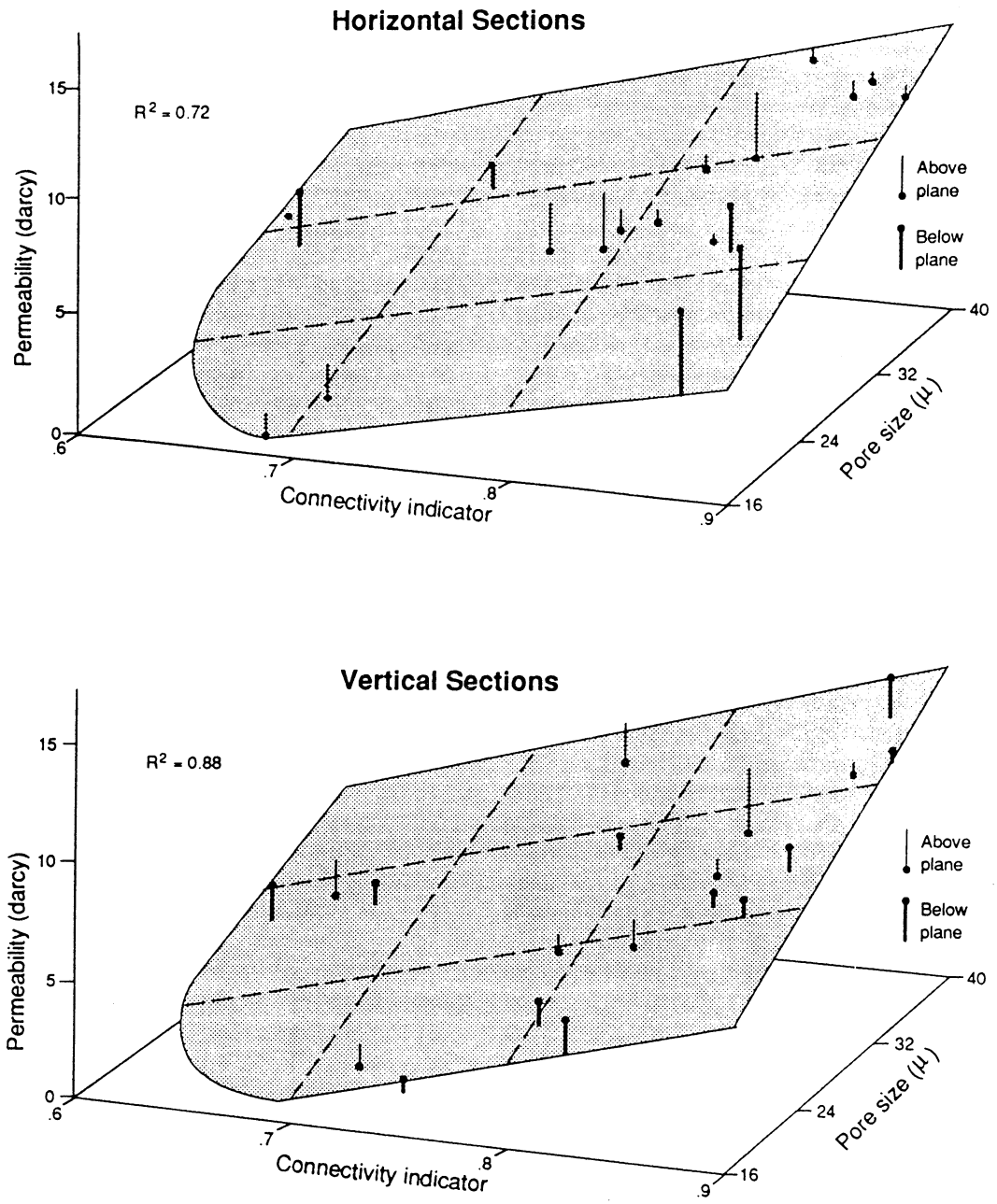

Figure 7.- Regression surfaces with pore size and connectivity as independent variables, and permeability as dependent variable. Solid circles are the data projected on the surfaces (predictions) and vertical lines indicate the distances between data points and their projections (residuals).

Table 1 lists the fractional amounts of each end member in each sample. These end member compositions can be plotted within a tetrahedron as a quaternary diagram (Figure 8) to show clearly the relationship between end member pore types and lithofacies. From Table 1 and Figure 8, end member one is present in significant amounts in the blocky channel oil saturated sands, end member two exists in most samples, particularly in large amounts in the transition zone between the blocky channel and channel margin facies, end member three is closely associated with the blocky channel water sands, and end member four is a typical component of the channel margin sands. In general, a trend from end member one through end member two to end emeber four of decreasing pore size is closely related to the fining upward sequence, commonly found in a channel deposit, from blocky channel oil saturated facies to channel margin facies. The blocky channel water saturated sands are more affected by the diagenetic processes, therefore, a poorly connected pore network is formed due to the significant amount of diagenetic clays. Figure 5 summarizes the general relationship between characteristic pore systems and lithofacies for the reservoir.

In addition to the quantitative data, flow properties may also be qualitatively estimated from pore characteristics. For the oil saturated sands, the fining upward sequence reduces pore sizes as well as permeabilities towards the top of the reservoir. The high connectivity in the 2-D images of the oil-saturated blocky channel facies and transition zone indicates good 3-D connectivity and large pore throats in the pore system. This favors low residual oil saturation and low capillary pressure. The channel margin facies appears to be characterized by less connected small pores. This is probably a result of small pore throats below the resolution of the imaging system, instead of a low 3-D connectivity. Good connectivity would favor low residual oil saturation; on the other hand, small pore throats may result in a high capillary pressure. Partial cementation in the water saturated zone has lowered the pore connectivity and permeability. The water saturated blocky channel facies and the transition zone have similar of permeabilities; however, their relative permeability may be very different as a result of the significant differences in pore size and connectivity.

Conclusions

This study has shown that the petrographic image analysis can effectively obtain the pore size and connectivity information, and the information can be closely related to flow properties, such as permeability. The unmixing procedure identifies pore end members which improve the understanding of the relationship between pore types and lithofacies. As a result, image analysis has allowed for the prediction of permeability values where no measurements were available and the extension of flow parameters to areas in the reservoir where only geological information was available. Therefore, the petrographic image analysis can be used not only as a tool to measure the flow properties of reservoir rocks but also as a link between geological information and reservoir characterization.

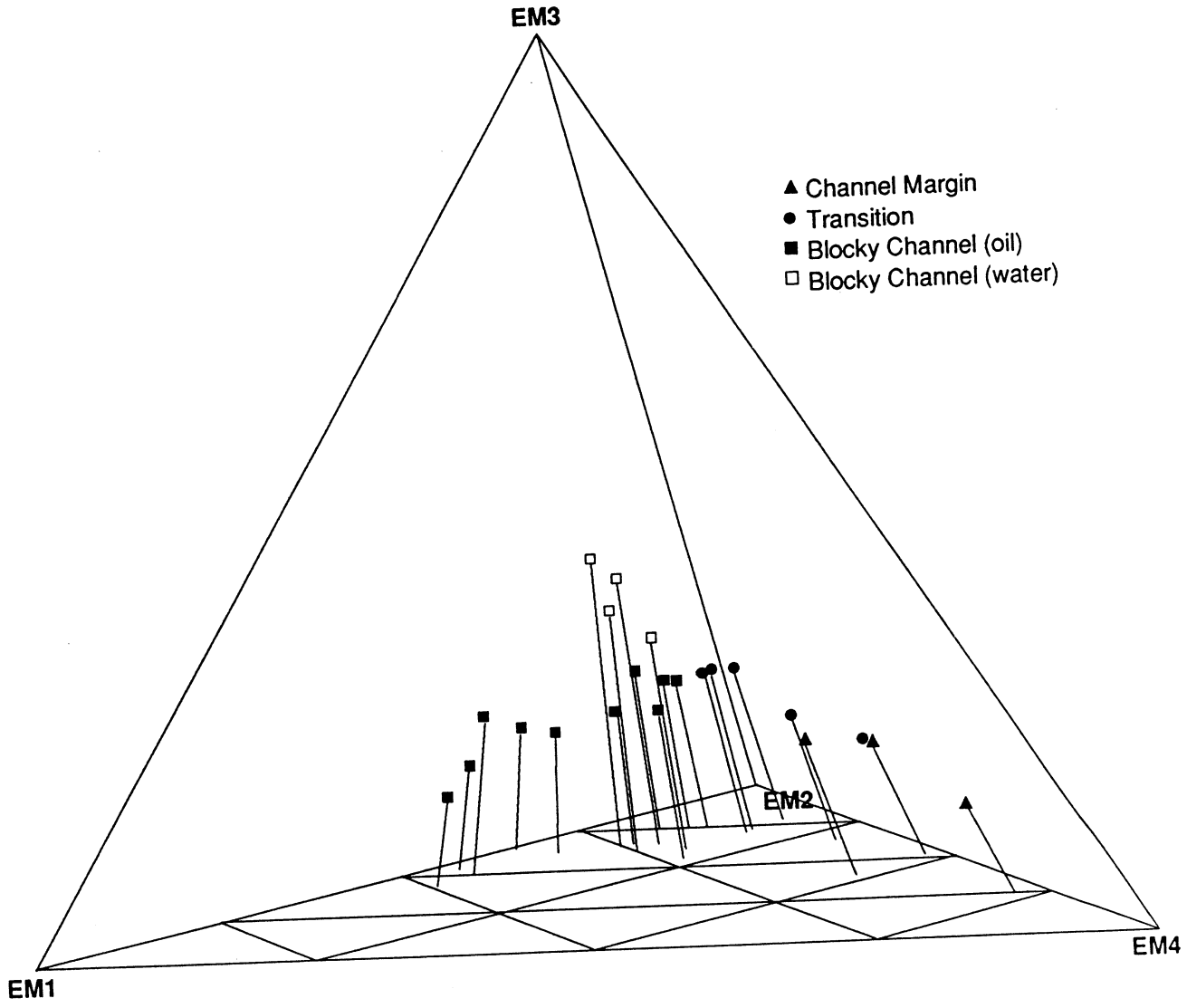

Figure 8.- Quaternary plot of sample compositions and their lithofacies. Values from vertical and horizontal thin sections are averaged and then plotted for each sample.

ACKNOWLEDGMENTS

The author would like to thank the Alberta Research Council, The Alberta Oil Sands Technology and Research Authority, and the Alberta Department of Energy for financially sponsoring this research program and for allowing us to publish these results. I would also like to thank John W. Kramers for his help throughout the study; Dave Cuthiell for his plotting program and discussions; Stefan Bachu for useful suggestions; Robert Ehrlich for valuable comments; and Max Baaske for laboratory support.

REFERENCES

Berryman, J.G. and Blair, S.C., 1987, Kozeny-Carman Relations and Image Processing Methods for Estimating Darcy's Constant: Journal of Applied Physics, v. 62, no. 6, p. 2221-2228.

Crabtree, S.J., Yuan, L., and Ehrlich, R., 1989, A Fast and Accurate Erosion-Dilation Method Suitable for Microcomputers, submitted to Computer Vision, Graphics, and Image Processing.

Cuthiell, D.L., Bachu, S., Kramers, J.W., and Yuan, L-P., in press, Characterizing Shale Clast Heterogeneities and Their Effect on Fluid Flow, in Proceedings of "The Second International Reservoir Characterization Conference", Dallas, June 25-28, 1989.

Delfiner, P., 1972, A Generalization of the Concept of Size: Journal of Microscopy, v. 95, p. 203-216.

Doyen, P.M., 1988, Permeability, Conductivity, and Pore Geometry of Sandstone: Journal of Geophysical Research, v. 93, No. B7, p. 7729-7740.

Ehrlich, R., Kennedy, S.K., Crabtree, S.J., and Cannon, R.L., 1984, Petrographic Image Analysis, 1, Analysis of Reservoir Pore Complexes: Journal of Sedimentary Petrology, v. 54, p. 1365-1378.

Ehrlich, R. and Davies, D.K., 1989, Image Analysis of Pore Geometry: Relationship to Reservoir Engineering and Modeling, SPE paper 19054, presented at the 1989 SPE Gas Technology Symposium, Dallas, June 7-9, 16 p.

Feret, L.R., 1931, La Grosseur des Grains des Matieres Pulverulentes: Association Internationale pour l'Essai des Materiaus, v. 2D, p. 428.

Full, W.E., Ehrlich, R., and Kennedy, S.K., 1984, Optimal Configuration and Information Content of Sets of Frequency Distributions: Journal of Sedimentary Petrology, v. 54, p. 117-126.

Full, W.E., Ehrlich, R., and Klovan, J.E., 1981, EXTENDED QMODEL - Objective Definition of External End Members in the Analysis of Mixtures: Mathematical Geology, v. 13, p. 331-344.

Gies, R.M., 1987, An Improved Method for Viewing Micropore Systems in Rocks With the Polarizing Microscope: SPE Formation Evaluation, v. 2, p. 209-214.

Kramers, J.K., Bachu, S., Cuthiell, D.L., Prentice, M.E. and Yuan, L.P., 1989, A multidisciplinary approach to reservoir characterization: the Provost Upper Mannville B Pool: Journal of Petroleum Technology, v. 28, p. 48-58.

Matheron, G., 1967, Elements pour une Theorie des Milieux Poreux: Paris,

Masson, 168p.

Parker, J.R., 1988, A Faster Method for Erosion and Dilation of Reservoir Pore-Complex Images: Canadian Journal of Earth Sciences, V. 25, No. 7, p. 1128-1131.

Rink, M., 1976, A Computerized Quantitative Image Analysis Procedure for Investigating Features and an Adapted Image Process: Journal of Microscopy, v. 107, p. 267-286.

Rink, M. and Schopper, J.R., 1978, On the Application of Image Analysis to Formation Evaluation: The Log Analyst, v. 19, p. 12-22.

Ruzyla, K., 1986, Characterization of Pore Space by Quantitative Image Analysis, SPE Formation Evaluation, v. 1, p. 389-398.

Scheidegger, A.E., 1960, The Physics of Flow through Porous Media, Rev. edition, University of Toronto Press, 313 pp.

Serra, J., 1982, Image Analysis and Mathematical Morphology: New York, Academic Press, 610p.

Wadell, H., 1932, Volume, Shape and Roundness of Rock Particles: Journal of Geology, v. 40, p. 443.

Walsh, J.B. and Brace, W.F., 1984, The Effect of Pressure on Porosity and the Transport Properties of Rock: Journal of Geophysical Research, v. 89 p. 9425-9431.

Yuan, L., in press, Image Analysis of Pore Size Distribution and Its Application: Proceedings of the Colloquium on "Statistical Applications in the Earth Sciences", Geological Survey of Canada, Paper 89-9.